Resonant photoelectron and photoelectron diffraction across the Fe L_3 edge of Fe_3O_4

H. Magnan,[1,*] P. Le Fèvre,[2] D. Chandesris,[2] P. Krüger,[3] S. Bourgeois,[3] B. Domenichini,[3] A. Verdini,[4] L. Floreano,[4] and A. Morgante[4,5]

[1]*CEA, DSM, IRAMIS, SPCSI, F-91191 Gif-sur-Yvette Cedex, France*

[2]*Synchrotron SOLEIL, L'Orme des Merisiers, Saint-Aubin, F-91192 Gif-sur-Yvette Cedex, France*

[3]*Institut Carnot de Bourgogne, BP 47870, F-21078 Dijon Cedex, France*

[4]*CNR-INFM Laboratorio Nationale, TASC, Bazovizza SS-14, Km 163.5, I-34012 Trieste, Italy*

[5]*Dipartimento di Fisica, Universita di Trieste, Via Valerio 2, 34127 Trieste, Italy*

(Received 16 November 2009; revised manuscript received 25 January 2010; published 24 February 2010)

We combined measurements of valence-band photoemission and valence-band photoelectron diffraction on Fe_3O_4 at the Fe $2p$-$3d$ resonance. The different structures in the valence band of magnetite due to the different sites of iron were identified experimentally. Specifically the structure near the Fermi level is unambiguously attributed only to octahedral Fe^{2+} sites (B-Fe^{2+}). We showed that tuning the photon energy to the resonance of B-Fe^{2+}, the whole valence band is dominated by signal coming from B sites of iron. Moreover this work shows how resonant photoelectron diffraction is a powerful tool for the study of mixed valence oxides.

DOI: 10.1103/PhysRevB.81.085121 PACS number(s): 71.20.−b, 79.60.−i, 61.05.js, 75.50.Bb

I. INTRODUCTION

Magnetite (Fe_3O_4) is one of the most fascinating materials. It is a room-temperature ferrimagnet of interest in applied magnetism, mineralogy, biology, geophysics, and paleomagnetism. Its potential application in spintronics has emerged since it has also been predicted to be half-metallic,[1] making it a promising candidate for high performance devices operating at 300 K and above. Fe_3O_4 crystallizes in the cubic inverse spinel structure,[2] in which the Fe cations are located either on tetrahedral sites (A sites) or on octahedral sites (B sites). At room temperature, one third of Fe atoms are located on A site as Fe^{3+}(A-Fe^{3+}), while the remaining two thirds of the Fe ions (with a formal valence $Fe^{2.5+}$) reside in B sites (B-Fe^{2+} and B-Fe^{3+}). An ordering of Fe^{2+} and Fe^{3+} in B sites was proposed to explain the Verwey transition[3] at about 120 K from a metallic ferrimagnet to an insulator.[2] The detailed nature of electronic structure[4] and the existence of charge and orbital ordering[5–9] are still being debated.

High-energy valence-band (VB) photoemission is a well-suited technique for the study of bulk electronic structure since the band dispersion effects can be considered negligible and the enhanced depth allows access to the bulk.[10,11] In resonant condition, i.e., using photon energies corresponding to core edge absorption transitions, it becomes a powerful method to unravel different electronic structure configurations thanks to chemical and site selectivity in x-ray absorption.[12] Moreover, x-ray photoelectron diffraction (XPD) from core level is a well-known technique to probe the local crystallography around selected species. Recently XPD from valence state was performed in resonant conditions at the reduced TiO_2(110) surface[13] and allowed to measure the charge distribution of the defect states.

In this paper, we present a study of the electronic structure of Fe_3O_4 by resonant VB photoemission and resonant XPD on the VB. Magnetite is here a prototype of oxide with three distinct species for the cation (A-Fe^{2+},B-Fe^{2+},A-Fe^{3+}). In this compound, the Fe^{2+} and Fe^{3+} components of the Fe $2p$ photoemission spectra can be hardly disentangled because of their large width (>1 eV) and small splitting,[14,15] thus hampering a reliable structural investigation by standard XPD. However, the contribution of each of these three species is remarkably well separated in magnetic circular dichroism (MCD).[16] The MCD spectra shows three sharp peaks (**a**,**b**,**c**) about 1 eV apart (708, 709, and 710 eV), which were assigned to the B-Fe^{2+}, A-Fe^{3+}, and B-Fe^{3+} ions, respectively. The contribution of these three species are strongly mixed in the valence-band photoemission, but Chen *et al.*[17] have shown that resonant excitation with photon energies **a**, **b**, or **c** significantly enhances the contribution of the corresponding ion in the valence band. In order to separate as much as possible the signals of the three Fe species, we have therefore carried out resonant photoemission experiments at the energies **a**, **b**, and **c**. Furthermore, we have measured XPD from the valence band in resonant and nonresonant conditions. The analysis shows that these combined techniques allow to unravel the contribution of the different electronic configurations in the valence-band photoemission of complex compounds showing different oxidation states of the same ion.

Some time ago it has been argued on the basis of resonant x-ray scattering (RXS) experiments, that at room temperature, all Fe ions on B sites are electronically equivalent[5] on time scales as short as 10^{-16} s in contradiction to the ionic picture and the peak assignment of the x-ray MCD experiments in Ref. 16. The time scale of the present resonant photoemission experiments is given by the life time of the Fe $2p3/2$ hole, i.e., about 10^{-15} s. Thus all Fe-B sites would be equivalent according to the argument of Ref. 5. It is not fully clear, however, in how far conclusions from RXS experiments, which relies on coherence between different cation sites, can be applied to resonant photoemission experiments which is a pure single-site process. For simplicity we shall interpret our data within the conventional ionic picture with species A-Fe^{2+}, B-Fe^{3+}, and B-Fe^{2+}. These ionic charges are formal ones and it is clear that the actual charges (and charge differences) are considerably smaller. In the end of Sec. IV we briefly discuss the implications of a scenario

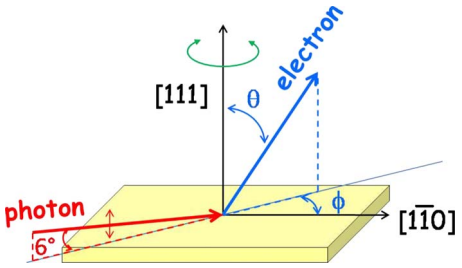

FIG. 1. (Color online) Geometry of the XPD experiment. The *p*-polarized light is impinging on the sample at grazing incidence (6°). The sample moves with azimuthal angle ϕ. The electron analyzer moves with the polar angle θ.

where all *B*-Fe ions have the same charge as suggested in Ref. 5.

The paper is organized as follows. In the next section, we describe the experimental details. Resonant photoemission is presented and discussed in Sec. III. The results and analysis of resonant XPD are presented and discussed in detail in Sec. IV, followed by conclusions.

II. EXPERIMENTAL APPROACH

15-nm-thick Fe_3O_4 (111) layer was grown in a dedicated setup[15,18] by atomic oxygen assisted molecular beam epitaxy on α-Al_2O_3(0001) substrate as described in details elsewhere.[19] The structure and the stoichiometry of the iron oxide film were checked *in situ*, respectively, by reflection high-energy electron diffraction and x-ray photoelectron spectroscopy (XPS). Resonant measurements require the use of synchrotron radiation and thus air exposure of the sample between preparation and resonant photoemission and photoelectron diffraction experiments. Great care has thus been taken in order to avoid eventual phase changes. After introducing the sample in the measurement chamber, we checked the cleanliness and the stoichiometry of the Fe_3O_4 layer by XPS. Only carbon contamination was observed, and it was successfully removed by annealing the sample during ~3 h at ~700 K under a 10^{-8} mbar oxygen partial pressure. The XPS spectra showed that this procedure is efficient to retrieve a clean and stoichiometric sample.

The experiments were performed at the ALOISA beamline of the Elettra Synchrotron Light Source in Trieste, Italy.[20] All measurements were done at room temperature. The linearly polarized x-ray beam was impinging on the sample at a constant grazing angle of 6°, with the polarization in the scattering plane, i.e., *p*-polarization geometry (Fig. 1). XPS spectra in the 690–790 eV photon energy range were taken with a photon energy resolving power about 2000. The resonant valence-band spectra were recorded at normal emission using the 66 mm hemispherical analyzer, which electron energy resolution was set to 300 meV (pass energy=30 eV), yielding an overall experiment resolution of 470 meV. XPD patterns were taken by rotating the hemispherical analyzer in the scattering plane (polar rotation θ) for different values of the sample azimuthal orientation ϕ, at constant grazing angle (6°). The azimuthal angle ϕ is defined with respect to the [1$\bar{1}$0] direction of Fe_3O_4 (see Fig. 1). The XPD patterns were taken by scanning ϕ over 80° including both symmetry directions [1$\bar{1}$0] and [11$\bar{2}$]. The polar (emission) angle was scanned from 7° to 65° above the horizon. The corresponding (θ, ϕ) region was mapped at constant solid angle with a resolution step corresponding to half the angular acceptance (2°) of the 66 mm hemispherical analyzer. The resonant photoemission spectra and the resonant XPD were recorded using photons of energy around the L_3 edge of iron (710 eV). The absorption spectrum at the Fe L_3 edge is recorded in partial electron yield during the acquisition of resonant photoemission. The photon energy scale of the absorption spectra was calibrated *a posteriori* by exploiting the real time acquisition of the drain current on the multilayer coating of the last beamline mirror.

III. RESONANCE OF THE VALENCE BAND AT THE Fe L_3 EDGE

Resonant photoemission excited by photons with energy near the absorption threshold of a core level is a useful technique for the investigation of VB features in solids. Previous studies of VB resonant photoemission on Fe_3O_4 have been performed at the Fe 3*p* edge[21,22] or at the Fe 2*p* edge using circularly polarized photons.[17] Here we present resonant spectra of the valence band at the L_3 edge (Fe 2*p*) using photons with linear polarization. The mechanism of resonant photoemission is well known. In an atomic picture, it is caused by the final-state interference between direct photoemission from the 3*d* levels ($3d^n \rightarrow 3d^{n-1}+e$) and autoionization processes ($2p^6 3d^n \rightarrow 2p^5 3dn^{n+1} \rightarrow 2p^6 3d^{n-1}+e$) following the $2p \rightarrow 3d$ core excitation. The case of L_3 edge is particularly interesting since calculations have shown that the excitation of *B*-Fe^{2+}, *A*-Fe^{3+}, and *B*-Fe^{3+} are well separated in the absorption spectra (separation of about 1 and 0.6 eV).[17,23,24] Therefore, by carefully choosing the photon energy one can expect to enhance the photoelectron intensity selectively on a particular site.

Figure 2 gives a general view of the absorption curve at the Fe L_3 edge [Fig. 2(a)] as well as of the resonance of the VB of Fe_3O_4 around the Fe L_3 edge recorded at normal emission [Fig. 2(b)]. The spectra are plotted as a function of the binding energy (horizontal scale) and for the different photon energies across the Fe L_3 edge (vertical scale). The color scale gives the photoemission intensity at each point of this two-dimensional (2D) map. One clearly observes that the valence band strongly resonates at the Fe L_3 edge. Indeed, the global intensity is enhanced by a factor of twenty. Moreover, the different structures in the VB resonate at different photon energies. The structure near the Fermi level (at about 1 eV binding energy) is maximum at 707.5 eV although the structures at higher binding energy near 4.4 eV (6.6 eV) resonate at higher photon energy 708.9 eV (709.6 eV). The photoemission spectra recorded at these three photon energies are plotted on Fig. 3, and the constant initial state (CIS) spectra for three different binding energies (1.2, 4.4, and 6.6 eV) are plotted on Fig. 4 with the absorption spectrum. We first remark that these CIS spectra do not display the usual Fano profiles.[25] Instead of that, they show structures which compare well with those of the absorption spectrum. This

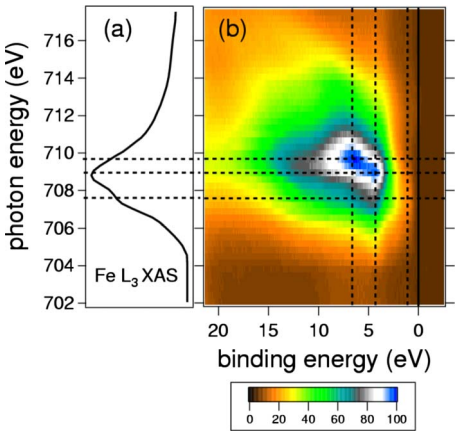

FIG. 2. (Color online) (a) experimental absorption spectrum at the Fe L_3 edge recorded in partial electron yield during the acquisition of resonant VB; (b) 2D plot of the resonant valence-band spectra recorded on Fe_3O_4 in p polarization. The spectra are plotted as a function of the binding energy (horizontal scale) and for the different photon energies across the Fe L_3 edge (vertical scale) with the same scale than in (a), the colors indicating the photoemission intensity as a function of these two variables. Vertical dashed lines indicate the position of 1.2, 4.4, and 6.6 eV binding energy. Horizontal lines indicate the position of 707.5, 708.9, and 709.6 eV photon energy.

must be due to a weak interference regime between photoemission and autoionization with a large predominance of the latter process.

We will first discuss the resonance behavior of the structure situated at 1.2 eV binding energy. According to calculations,[17,26,27] this structure is expected to be only due to B-Fe^{2+}. On Fig. 4, we see that it resonates at a photon energy about 1.1 eV below the maximum of the absorption. Kuiper *et al.*,[16] as well as Mirone *et al.*,[24] have calculated the site-resolved contributions to the total absorption in Fe_3O_4 using the crystal field multiplet approach. The spectra of Ref. 24 are reproduced in Fig. 4. It can clearly be observed that

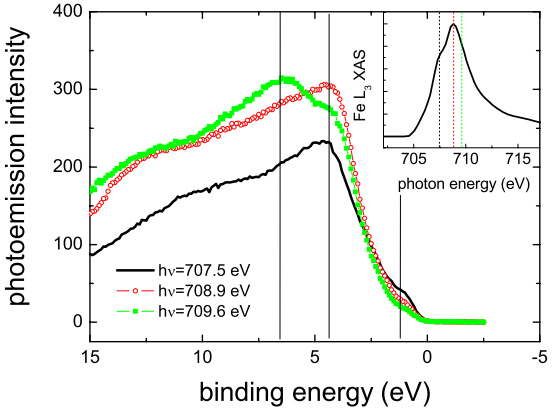

FIG. 3. (Color online) Valence band recorded at different photon energies 707.5 eV (black line), 708.9 eV (red open circles), and 709.6 eV (green squares). Vertical lines indicate the position of 1.2, 4.4, and 6.6 eV binding energy. Inset: absorption curve at the Fe L_3 edge. Dashed vertical lines indicate the position of 707.5, 708.9, and 709.6 eV photon energy

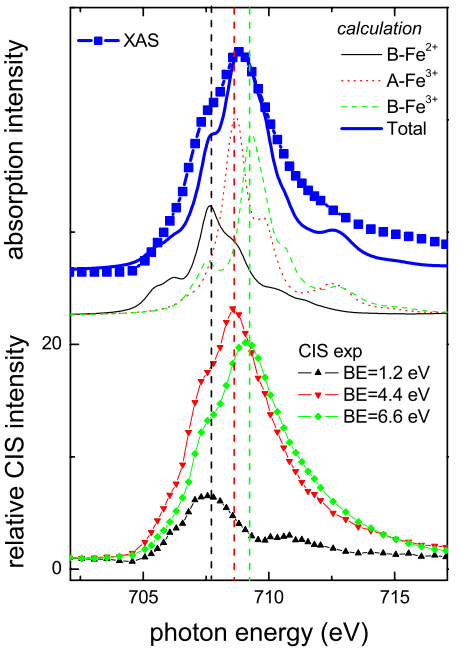

FIG. 4. (Color online) Bottom part: experimental VB-CIS spectra recorded on Fe_3O_4 at the Fe L_3 edge for 1.2 eV (black up-triangle), 4.4 eV (red down-triangle), and 6.6 eV (green squares) binding energies. The CIS spectra are normalized to the intensity at 705 eV. Top part: experimental absorption spectrum (blue squares) and calculations of site-resolved contributions to the absorption spectrum of Fe_3O_4 from Ref. 24 for B-Fe^{2+} (black solid line), A-Fe^{3+} (red dotted line), B-Fe^{3+} (green dashed line), and total absorption (solid blue line). Vertical lines indicate the position of the maximum of the three CIS spectra.

the calculation of B-Fe^{2+} absorption reproduces well the resonance of the 1.2 eV binding energy VB structure both for the shape and for the photon position. We can then conclude that this structure is only due to B-Fe^{2+} species.

We can also compare the CIS spectra of the two other structures with Mirone *et al.* calculations. The second structure (with a binding energy of 4.4 eV) is maximum at a photon energy 0.2 eV below the maximum of the absorption, at the energy of maximum of absorption of A-Fe^{3+}. However, the CIS spectrum presents also a bump at lower photon energy, at the energy of maximum absorption of B-Fe^{2+}. The third structure (at 6.6 eV binding energy) presents also two resonances, the main one is at the maximum of B-Fe^{3+} absorption and the lower one at the energy of maximum absorption of B-Fe^{2+}. These two CIS spectra are also larger than the calculation. We can therefore conclude that these VB structures are mainly due to A-Fe^{3+} and B-Fe^{3+} respectively but they have also a contribution of B-Fe^{2+} species. These findings have been predicted by Chen *et al.* calculations[17] which show that 4 and 6 eV binding energies correspond to $^5T_2$ multiplet for A-Fe^{3+} and B-Fe^{3+} respectively, but at these binding energies there is also a contribution of B-Fe^{2+}. We can notice that the experimental binding energies determined in the present work compare well with Chen *et al.* calculations[17] but that they are ~2 eV higher than those derived by band structure calculations.[26,27] Let us note that the calculations in Ref. 24 were done for an electric

field in the surface plane whereas the present experiments are performed with out-of-plane polarization. Nevertheless we believe that the comparison with these calculations is justified, since the polarization dependence of the L_3 absorption (linear dichroism) is much smaller than the site dependence, as can be inferred from Ref. 16 where two orthogonal in-plane polarizations were compared.

As a conclusion, resonant photoemission experiment and constant initial state measurements allowed us to identify the structures in the VB of Fe_3O_4. We have clearly shown that the structure near the Fermi level is only due to B-Fe^{2+} species. The structures around 4 and 6 eV binding energy resonate at the maximum of absorption of A-Fe^{3+} and B-Fe^{3+}, respectively, but these structures are due to mixed contributions. These results have been already suggested from previous resonant experiment[21,22] performed at the Fe $3p$ edge. However, identification of VB structure at the $3p$-$3d$ resonance is more difficult since resonances are broader and less intense.

IV. RESONANT PHOTOELECTRON DIFFRACTION ON VALENCE BAND

The selective amplification, in the valence band, of the contribution of the different iron species in Fe_3O_4 compound offers the opportunity to probe the environment of each iron ion separately, thanks to resonant photoelectron diffraction. Photoelectron diffraction from core levels is a powerful technique for determining structural properties on single-crystal surfaces. Moreover, if the crystal structure is known, XPD can be used for assigning an electronic structure to a particular site. Recent papers[13,28] have shown that XPD can be also used in resonant conditions in order to increase the intensity of the measured peak.

Here, we have performed resonant XPD of the valence band of Fe_3O_4. By choosing a resonant energy, we aimed at obtaining a XPD pattern associated with a specific species. A site and B site iron should be easily discriminated, since these two sites should give different photoelectron diffraction patterns.

More precisely, we have recorded XPD on the VB of Fe_3O_4 at three different photon energies: 692 eV, before the L_3 edge of iron [denoted *or* (off resonance)], 707.5 eV at the maximum of the B-Fe^{2+} absorption (denoted **a**) and 709 eV at the maximum of the A-Fe^{3+} absorption (denoted **b**). Special care has been taken concerning the stability of the photon energy during experiment and it was better than 0.1 eV. Experimental XPD are plotted on Figs. 5(a)–5(c). They are reported as χ functions, where $\chi(\theta,\phi)=[I(\theta,\phi)-I_0(\theta)]/I_0(\theta)$. Here, $I(\theta,\phi)$ is the integration of the VB absolute intensity between the Fermi level and 8.5 eV binding energy and $I_0(\theta)$ a smooth background obtained by a polynomial fitting of the azimuthal average of $I(\theta,\phi)$.[29]

We have simulated the XPD patterns using multiple scattering calculations with the EDAC code.[30] For the simulation, we have only used the Fe $3d$ level, since the cross section of oxygen $2p$ is low at this photon energy (around 710 eV). Fe_3O_4 is modeled with a spherical cluster which contains 331 atoms (cluster radius 9.5 Å). We used the lattice

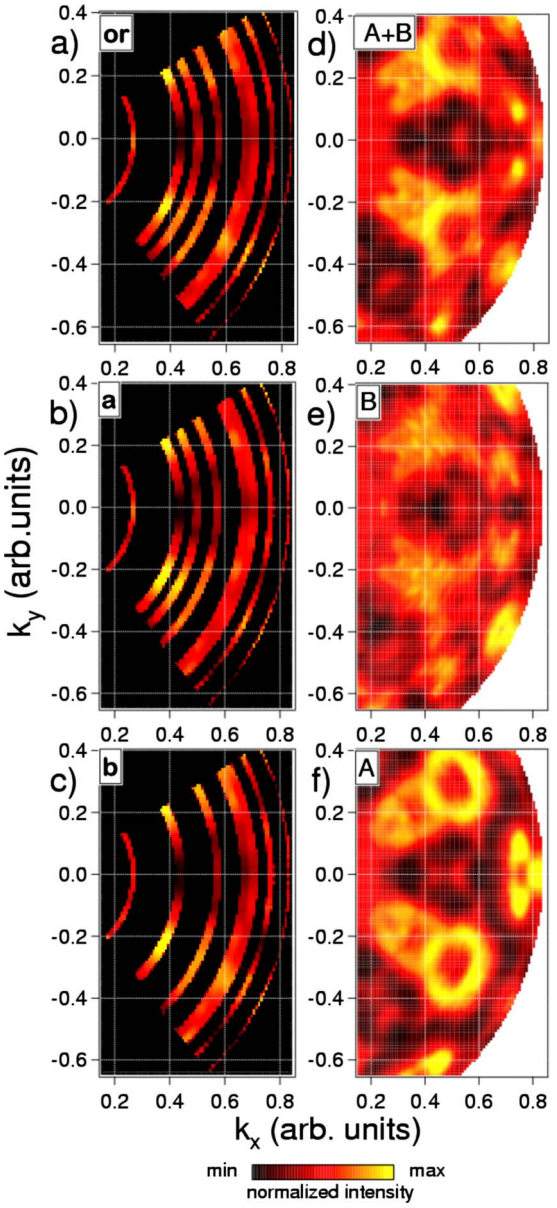

FIG. 5. (Color online) left: experimental VB photoelectron diffraction (between 0 and 8.5 eV binding energy) on Fe_3O_4 recorded with photon energy of (a) 692, (b) 707.5, and (c) 709 eV. Black color corresponds to angles where no data was recorded. right: multiple scattering calculations of XPD of Fe_3O_4 using EDAC code (see text) for Fe $3d$ level and (d) for all the iron sites, (e) the B sites of iron, and (f) the A sites of iron. The representation is a projection of diffraction intensity onto the plane of the paper, the scale is $\sin(\theta)$ and $\phi=0$ is found at three o'clock and corresponds to $[1\bar{1}0]$ direction of Fe_3O_4.

parameter of bulk magnetite[2] and an incident angle of the photons (p polarized) of 85°. We considered the emission of the 24 different iron atoms in the lattice and the results presented here are the sum of these contributions. By a test performed on Fe $3p$ XPD recorded with the same kinetic energy as here (not shown here), we have determined the best parameters for the simulation and found that a mean-free path of 10 Å and multiple scattering up to seventh order can well reproduce the data. Moreover we find that ampli-

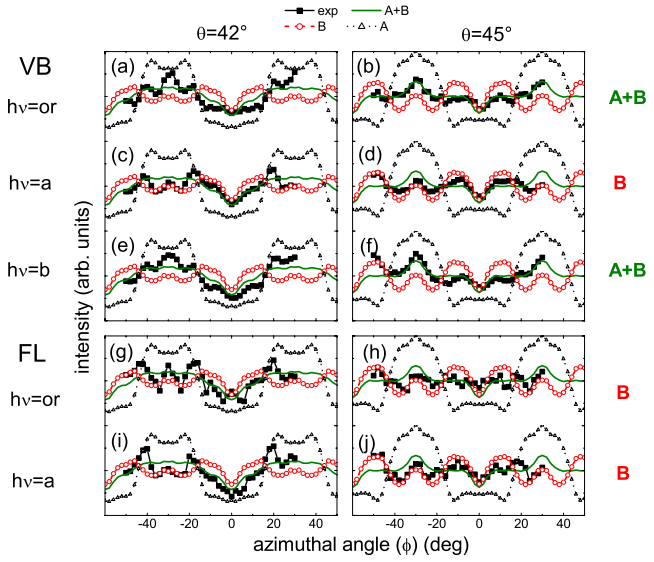

FIG. 6. (Color online) experimental azimuthal scans (black squares) recorded at θ=42° (left column) and at θ=45° (right column) with photon energy indicated on the left (or=692 eV, a =707.5 eV, and b=709 eV). The signal is the integration of the VB absolute intensity (a)–(f) from the Fermi level to 8.5 binding energy and (g)–(j) from Fermi level to 1.5 eV. Comparison with multiple scattering calculations for all sites of iron (green line) for B-sites of iron (red circles) and for A sites of iron (black triangles). The best model for each case is indicated on the right of the figure.

tudes calculated by EDAC are much larger than experimental ones since calculations don't take into account thermal and structural disorder. But we determined that dividing EDAC calculations by a factor 3.7 can well correct the amplitudes. Three different calculations are plotted on Figs. 5(d)–5(f) considering emission of all (d) Fe atoms, (e) emission of Fe atoms situated in B sites, and (f) emission of Fe atom situated in A sites. For a direct comparison with experimental data, the calculations have been symmetrized with respect to $[1\bar{1}0]$ direction in order to take into account the two 60° variants of Fe_3O_4 deposited on alumina. Moreover, the calculation is normalized in the same manner as the experimental data.

One can see on Fig. 5 that the simulations reproduce well the main feature of experimental data: low intensity at ϕ =0° for polar angle between θ=20° and θ=35° and higher intensity at ϕ= ± 30°. Comparing the different models, it can be seen that the main difference in XPD between A-site emitter and B-site emitter is for θ around 40–45°. Therefore, on Fig. 6 we compare experimental data with the different models by plotting the azimuthal scans at θ=42° and θ=45°. For a direct comparison of experimental data and calculations, EDAC calculations were divided by the factor 3.7 determined above.

We will first discuss the results concerning the integration of the VB up to 8.5 eV [Figs. 6(a)–6(f)]. One clearly sees that for off resonance (or), the best simulation is obtained by taking into account all the possible iron sites, as it was expected. This is also the case when using a photon energy at the maximum of A-Fe^{3+} absorption (**b**). However, when the photon energy is tuned to **a** energy, the signal is better simulated by considering only B sites. We have already shown (part III) that at this photon energy, the spectral structures due to B-sites resonate, here we evidence that the resonance of B sites is sufficiently large to dominate all the VB.

On Figs. 6(g)–6(j), we have also plotted the azimuthal scans of the intensity of the VB near the Fermi level (from integration up to 1.5 eV binding energy), for photon energies or/and **a**. This part of VB is due to B-Fe^{2+}, according to our resonant experiment (see part III) and calculations.[17,26,27] For these two cases, the XPD experiment confirm this result, the data being well reproduced by considering only B sites.

As a conclusion, resonant XPD experiments allow to unravel the resonance behavior of Fe_3O_4 VB. We evidence experimentally that the structure near the Fermi level is only due to B sites of iron. These findings are consistent with theoretical predictions.[17,26,27] We showed that tuning photon energy to the resonance of B-Fe^{2+}, the whole VB is dominated by signal coming from B sites of iron. However when the photon energy is at the resonance of A-Fe^{3+}, these sites do not dominate the signal. The comparison with calculations reveals that the contribution of A sites at this energy is the same as at out of resonance, i.e., only 1/3 of the signal. The calculations by Mirone *et al.*[24] show that the L_3-absorption spectra of the three species overlap considerably (see Fig. 4). We can estimate that at 709 eV (energy **b**) the contribution of A-Fe^{3+} is about 50% of the total absorption, although the measured contribution with resonant XPD is much lower (about 30%). This phenomenon of strong mixture between the different sites at energy **b** has also been observed in magnetic circular dichroism resonance[17] and the authors claim that, above energy **a**, incoherent Auger electrons contribute to the background of VB, and thus increase the contribution of B sites.

This result shows the advantages and the limitations of the resonant XPD method. We have clearly confirmed that resonance can be used to enhance a particular electronic structure in order to allow XPD measurements as it was already used in previous work concerning TiO_2 defect peak.[13,28] Moreover, when different contributions are mixed in the VB, resonance can be also used to enhance only one particular contribution but only in some cases. The photon energies of resonances must be well separate or one can only use the resonance which has the lower photon energy. Obviously, this result can be generalized to other compounds, such as other oxides with mixed valence or with various stoichiometries.

We now briefly discuss the possibility that all Fe ions on B sites are equivalent, so that there is only a single B-Fe species (with formal charge +2.5) as argued by some authors.[5] If this is the case, the valence-band features can obviously no longer be assigned to different charge states of the Fe ions but only to the two different crystallographic sites (A-Fe,B-Fe). Our assignments in Sec. III should then be understood in such a restricted way. As for the photoelectron diffraction data of Sec. IV, the data has been analyzed in purely structural terms i.e., the assignments in Fig. 6 are to crystallographic sites A and B alone and independent of the Fe valency. This analysis remains valid even if all B-Fe ions are equivalent. For the same reasons, the resonant XPD experiment is not sensitive to charge order. It can thus be ex-

pected to yield identical results above and below the Verwey transition temperature, irrespectively of whether there is charge ordering of Fe-*B* sites or not.

V. CONCLUSION

We have combined resonant VB photoemission and resonant photoelectron diffraction experiments on Fe_3O_4 at the Fe L_3 edge. This allowed us to unravel the VB of magnetite by assigning the main spectral features to the three different Fe species. In particular the structure near the Fermi level could unambiguously be attributed to the *B*-Fe^{2+} ions. Our study illustrates the power of the resonant XPD technique for decomposing the VB into contributions from sites with different valency and symmetry, even when these contributions strongly overlap.

ACKNOWLEDGMENTS

We wish to thank S. Gota for providing us the data of absorption calculation on Fe_3O_4 published in Ref. 24. The European Commission is gratefully acknowledged for the access to Elettra facilities (Contract No. RII3-CT-2004-506008). Moreover, this work has benefited from financial support by the French National Research Agency (ANR) through the project "Development of resonant photoelectron diffraction (RPED)."

*hmagnan@cea.fr; http://iramis.cea.fr/en/

[1] A. Yanase and K. Siratori, J. Phys. Soc. Jpn. **53**, 312 (1984).
[2] N. Tsuda, K. Nasu, A. Yanase, and K. Siratori, *Electronic Conduction in Oxides* (Springer-Verlag, Berlin, 1991).
[3] E. J. W. Verwey and K. Siratori, Nature (London) **144**, 327 (1939).
[4] M. J. Wenzel and G. Steinle-Neumann, Phys. Rev. B **75**, 214430 (2007).
[5] J. García, G. Subias, M. G. Proietti, H. Renevier, Y. Joly, J. L. Hodeau, J. Blasco, M. C. Sanchez, and J. Berar, Phys. Rev. Lett. **85**, 578 (2000).
[6] E. Nazarenko, J. E. Lorenzo, Y. Joly, J. L. Hodeau, D. Mannix, and C. Marin, Phys. Rev. Lett. **97**, 056403 (2006).
[7] J. E. Lorenzo, C. Mazzoli, N. Jaouen, C. Detlefs, D. Mannix, S. Grenier, Y. Joly, and C. Marin, Phys. Rev. Lett. **101**, 226401 (2008).
[8] J. Schlappa *et al.*, Phys. Rev. Lett. **100**, 026406 (2008).
[9] J. García, G. Subias, J. Herrero-Martin, J. Blasco, V. Cuartero, M. Concepcion Sanchez, C. Mazzoli, and F. Yakhou, Phys. Rev. Lett. **102**, 176405 (2009).
[10] P. Le Fèvre, H. Magnan, D. Chandesris, J. Jupille, S. Bourgeois, A. Barbier, W. Drube, T. Uozumi, and A. Kotani, Nucl. Instrum. Methods Phys. Res. A **547**, 176 (2005).
[11] D. Schrupp, M. Sing, M. Tsunekawa, H. Fujiwara, S. Kasai, A. Sekiyama, S. Suga, T. Muro, V. A. M. Brabers, and R. Claessen, Europhys. Lett. **70**, 789 (2005).
[12] P. Le Fèvre, J. Danger, H. Magnan, D. Chandesris, J. Jupille, S. Bourgeois, M.-A. Arrio, R. Gotter, A. Verdini, and A. Morgante, Phys. Rev. B **69**, 155421 (2004).
[13] P. Krüger *et al.*, Phys. Rev. Lett. **100**, 055501 (2008).
[14] J. F. Anderson, M. Kuhn, and U. Diebold, Surf. Sci. Spectra **4**, 266 (1996).
[15] S. Gota, J. B. Moussy, M. Henriot, M. J. Guittet, and M. Gautier-Soyer, Surf. Sci. **482-485**, 809 (2001).
[16] P. Kuiper, B. Searle, L.-C. Duda, R. Wolf, and P. van der Zaag, J. Electron Spectrosc. Relat. Phenom. **86**, 107 (1997).
[17] J. Chen, D. J. Huang, A. Tanaka, C. F. Chang, S. C. Chung, W. B. Wu, and C. T. Chen, Phys. Rev. B **69**, 085107 (2004).
[18] S. Gota, E. Guiot, M. Henriot, and M. Gautier-Soyer, Phys. Rev. B **60**, 14387 (1999).
[19] J.-B. Moussy *et al.*, Phys. Rev. B **70**, 174448 (2004).
[20] L. Floreano *et al.*, Rev. Sci. Instrum. **70**, 3855 (1999).
[21] Y. Q. Cai, M. Ritter, W. Weiss, and A. M. Bradshaw, Phys. Rev. B **58**, 5043 (1998).
[22] R. J. Lad and V. E. Heinrich, Phys. Rev. B **39**, 13478 (1989).
[23] J. P. Crocombette, M. Pollak, F. Jollet, N. Thromat, and M. Gautier-Soyer, Phys. Rev. B **52**, 3143 (1995).
[24] A. Mirone, M. Sacchi, and S. Gota, Phys. Rev. B **61**, 13540 (2000).
[25] U. Fano, Phys. Rev. **124**, 1866 (1961).
[26] Z. Zhang and S. Satpathy, Phys. Rev. B **44**, 13319 (1991).
[27] H.-T. Jeng and G. Y. Guo, Phys. Rev. B **65**, 094429 (2002).
[28] P. Krüger, S. Bourgeois, B. Domenichini, H. Magnan, D. Chandesris, P. Le Fèvre, L. Floreano, A. Cossaro, A. Verdini, and A. Morgante, Surf. Sci. **601**, 3952 (2007).
[29] A. Verdini, A. Cossaro, L. Floreano, A. Morgante, A. Goldoni, D. Ghidoni, A. Sepe, S. Pagliara, and L. Sangaletti, Phys. Rev. B **77**, 075405 (2008).
[30] F. J. García de Abajo, M. A. Van Hove, and C. S. Fadley, Phys. Rev. B **63**, 075404 (2001).